Haidar Faisal Helal Mobark[1], Ali Hussein Al-Azzawi[2], Abdulraheem Kadhim AbidAli[3], Barhm Mohamad[4]*

COMPARATIVE TRIBOLOGICAL ANALYSIS OF Al-Fe-Si AND Al-Fe-Cr BASED ALLOYS

UPOREDNA TRIBOLOŠKA ANALIZA LEGURA TIPA Al-Fe-Si I Al-Fe-Cr

Adresa autora / Author's address:
[1] College of Agriculture, Al-Qasim Green University, Babel, Iraq
H.F.H. Mobark (iD) 0000-0001-6809-8452

[2] Department of Mechanical Engineering, College of Engineering, University of Misan, Misan, Iraq   A.H. Al-Azzawi (iD) 0000-0003-4402-6205
[3] College of Materials Engineering, University of Babylon, Babel, Iraq   A.K. AbidAli (iD) 0000-0001-8961-0339
[4] Department of Petroleum Technology, Koya Technical Institute, Erbil Polytechnic University, Erbil, Iraq   B. Mohamad (iD) 0000-0001-8107-6127   *email: barhm.mohamad@epu.edu.iq

Abstract

This study presents a comparative investigation of the tribological behaviour and microstructural characteristics of two different alloys, namely 77.3 % Al-1.8 % Fe-16.7 % Si and 54.1 % Al-12.8 % Fe-27.8 % Cr. High temperature alloys are fabricated by stir casting technique. Tribology analysis is conducted to assess wear, crack formation, and cavity zones for both alloys using Scanning Electron Microscopy (SEM). Additionally, optical micrography is employed to examine their microstructures. The results reveal significant differences between the two alloys, with the 77.3 % Al-1.8 % Fe-16.7 % Si alloy exhibiting higher Vickers hardness and superior wear resistance compared to the 54.1 % Al-12.8 % Fe-27.8 % Cr alloy. Optical micrographs confirm a well-defined grain distribution for the former alloy and a similar homogeneous microstructure for the latter.

Rezime

U ovom radu je predstavljeno uporedno istraživanje tribološkog ponašanja i mikrostrukturnih karakteristika dve različite legure, zapravo, 77,3 % Al-1,8 % Fe-16,7 % Si i 54,1 % Al-12,8 % Fe-27,8 % Cr. Visokotemperaturne legure se proizvode metodom vrtložnog livenja. Tribološka analiza se izvodi za procenu trošenja, formiranja prslina, i šupljih zona za obe legure, primenom skening elektronske mikroskopije (SEM). Pored toga, optička mikrografija se primenjuje za analizu mikrostruktura. Rezultati pokazuju značajne razlike između ovih legura, gde 77,3 % Al-1,8 % Fe-16,7 % Si legura pokazuje veću Vikers tvrdoću i izuzetnu otpornost na habanje u poređenju sa legurom 54,1 % Al-12,8 % Fe-27,8 % Cr. Optički mikrosnimci potvrđuju dobro definisanu raspodelu zrna u prvoj leguri, kao i sličnu homogenu mikrostrukturu kod druge legure.

INTRODUCTION

Tribology, the study of friction, wear, and lubrication of materials, has garnered significant interest in recent years, especially in the context of Al-Fe-Cr and Al-Fe-Si based alloys. These alloys are renowned for their excellent mechanical properties and potential applications in various industries. Their tribological behaviour has been the subject of extensive research, aimed at understanding their performance under different conditions. Researchers have explored the effects of alloy composition, heat treatment, and microstructural characteristics on friction and wear properties. Additionally, surface engineering techniques, such as coatings and treatments, have been investigated to enhance the tribological performance of these alloys. Aranda et al. /1/, studied the effect of Cr additions (1.0-5.0 wt.%) on Al-20Si-5Fe alloy using conventional solidification and suction casting. Suction casting improved microstructural homogeneity, transforming the Al3FeSi2 intermetallic to an acicular structure, which enhanced compressive plasticity (> 300 %) despite reduced hardness. The highest microhardness was 220 HV (5 wt.% Cr, conventional) and 192 HV (3 wt.% Cr, suction casting). Mahboobeh Azadi and Mohammad Azadi /2/, studied aluminium-silicon alloys reinforced with 1 wt.% Si and clay nanoparticles, prepared via stir casting and aging heat treat-

ment. Tribological properties, including hardness, wear rate, and friction coefficient, were analysed using Vickers hardness, pin-on-disk tribometre, and compression tests, with data processed via Design-Expert® software. A study conducted by Farsi et al. /3/ focused on the application of a high-gradient magnetic separation method for effective separation of weak magnetic particles, specifically in an industrial setting.

The researchers explored and implemented high-gradient magnetic separation techniques to address the challenges of separating weakly magnetic particles from complex mixtures in an industrial context. The study likely involved designing and testing a specialised magnetic separator to achieve efficient separation of these particles which have relatively low magnetic susceptibility compared to strongly magnetic materials. The application of this method could have practical implications in various industries where precise separation of weakly magnetic particles is essential for processing and product quality. The study presented experimental results, data analysis, and insights into the performance and efficiency of the high-gradient magnetic separation method. Al-Abboodi et al. /4/ present an evaluation of the mechanical properties of a metallic glass alloy (Fe49.7-Cr17.1-Mn1.9-Mo7.4-W1.6-B15.2-C3.8-Si2.4) prepared by spark plasma sintering using a three-point bending apparatus. The study achieved notch fracture toughness and Young's modu-

lus values of 231 GPa and 4.91 MPa√m, respectively, and found reliable results for Young's modulus using Vickers indentation measurements. The proposed method for examining micro-scale mechanical properties is applicable to samples with different compositions made by other means. Aldeen et al. /5/ investigates the effects of isothermal and isochronal aging on N36 zirconium alloy after β-quenching. The research involves characterisation using various microscopy techniques and spectroscopy to observe microstructure and second-phase particle (SPPs) evolution. The results reveal that the implemented quenching leads to a fine interlaced α-plates structure, and after aging, recrystallization occurs with non-uniform grains and a random SPPs distribution. Hardness declines with increasing temperature and time, while roughness and wettability increase with higher aging temperatures. Kang et al. /6/ explore the fabrication of Al-Fe-Cr quasicrystal-reinforced metal matrix composites using a laser powder bed fusion (LPBF) process. The LPBF-processed Al-Fe-Cr alloy exhibits a multiscale heterogeneous structure with nanosized Al-Fe-Cr quasicrystalline particles distributed in the α-Al columnar grain structure. The alloy demonstrates high mechanical strength due to the ultrafine multireinforced microstructure-induced Orowan strengthening effect, resulting in an ultimate tensile strength of 530.80 MPa, yield strength of 395.06 MPa, and elongation of 4.16 %. The fractographic analysis indicates a combination of ductile-brittle fracture as the dominant fracture mechanism. Zhang et al. /7/ focus on a specially designed Al-Fe-Cr alloy fabricated through a laser powder bed fusion (LPBF) process, resulting in a multi-scaled heterogeneous composite structure with high relative density and defect-free features. The LPBF-processed sample exhibits distinct composite structures in three regions: the inner laser fusion zone (LFZ) with ultrafine cellular structures containing spherical Al-Fe-Cr quasicrystals, the molten pool boundary (MPB) with coarse flower-like quasicrystal particles and rectangular θ-Al13(Fe,Cr)2-4 particles, and the heat-affected zone (HAZ) with finer reinforcements dispersed in the α-Al matrix. The tribological investigation shows the LPBF-processed sample has stable friction coefficients and higher wear resistance compared to other LPBF-processed Al alloys, with a duplex wear mechanism of adhesive and oxidation wear. Byron Blakey-Milner et al. /8/ is a thorough review of metal additive manufacturing in the aerospace industry, highlighting its significant commercial and performance advantages. The opportunities in this field include cost and lead time reductions, novel materials and unique design solutions, mass reduction through lightweight designs, and consolidation of components for improved performance and risk management. Various high-profile aerospace applications, such as rocket engines, propellant tanks, heat exchangers, turbomachinery, and satellite components, have already commercially benefited from metal additive manufacturing. The paper also addresses challenges and potential opportunities for using this technology in each application scenario.

Leyson et al. /9/ presents a quantitative, parameter-free model for predicting the flow stress of alloys containing substitutional solutes. The model utilizes density functional theory and a flexible-boundary-condition method to accurately describe the interaction energies between solutes and dislocations. It successfully predicts flow stresses for various Al alloys, including Al-Mg and Al-Mn, and agrees well with experimental results for quasi-binary Al-Cr-(Fe) and Al-Cu-(Fe) alloys. The model offers a basis for computational design of alloys, focusing on solute-strengthening mechanisms, and aligns with the 'stress equivalency' postulate of Basinski. In the study by Xi et al. /10/, near-fully dense Al-12Si matrix composites reinforced with TiB_2 ceramic particles (2 wt.%) are successfully fabricated using selective laser melting (SLM) and hot pressing (HP) techniques. The TiB_2 ceramic particles are homogeneously distributed in the Al-12Si matrix at the micrometre-scale due to excellent wetting between the molten alloy and ceramic. The microstructural analysis of the as-fabricated SLM samples show the formation of a supersaturated α-Al phase and the decrease of free residual Si compared to the hot-pressed ones. Both composites exhibited a fine microstructure with a grain size of ~5.1 μm and ~5.8 μm for SLM- and HP-fabricated samples with addition of TiB_2 ceramic particles. The SLM Al-12Si/TiB_2 composite exhibited significantly improved microhardness (~142±6.0 $HV_{0.05}$) and yield strength (~247± 4.0 MPa) compared to the corresponding HP one, attributed to the fine cell morphology and nanostructured dispersion strengthening achieved through the SLM process.

Kang et al. /11/ manufactured Al-Fe-Cr quasicrystal (QC) reinforced Al-based metal matrix composites through selective laser melting (SLM) from a powder mixture. Parametrical optimisation focused on laser scanning speed, resulting in an almost dense (99.7 %) free-crack sample with an ultrafine microstructure. A phase transition from decagonal QC Al65Cu25Fe10Cr5 to icosahedral QC Al91Fe4Cr5 was observed at lower laser scanning speeds. Differential scanning calorimetry curves revealed the QC phase's stability up to 500 °C. The study examined the effects of annealing temperature on microstructural and mechanical properties, indicating that QC particles prevent α-Al grain recrystallization and growth during annealing. However, the growth of QC particles resulted in a porous structure, improving Young modulus but reducing ductility. In Wang et al. /12/, an Al-1Fe (wt.%) alloy with nanosized Al_3Fe phase underwent continuous rheo-extrusion and heat treatment. The nanosized phase spheroidized during heat treatment, while coarsening and forming plate-like structures occurred with prolonged treatment. Tensile strength decreased slightly at 200 °C and 300 °C, but significantly at higher temperatures. However, the alloy's strength remained higher than the as-cast Al-Fe alloy throughout heat treatment. Khadem et al. /13/ conducted a review on multilayer coating systems for tribological applications. These coatings have been widely used to reduce friction and wear in mechanical systems, contributing to improved efficiency, reliability, and system lifespan. The paper focused on Ti-based and Cr-based coatings, exploring their materials, design concepts, mechanical properties, deposition methods, and friction and wear characteristics. Multilayer coatings offer the advantage of tailoring coating properties to suit specific operating conditions, making them highly versatile in various engineering applications. Aluminium alloys are essential materials in additive

manufacturing (AM), but they face challenges due to low laser absorption, high thermal conductivity, and reduced powder flowability, resulting in poor processability. Recent efforts have focused on developing new compositions specifically designed for laser-based powder bed AM. This review by Aversa et al. /14/ provides an overview of the state of the art, including microstructural and mechanical characterisations of these aluminium alloys used in laser powder bed fusion. Kotadia et al. /15/ discuss the growing interest in additive manufacturing (AM) of metallic alloys for structural and functional applications, revolutionizing design and manufacturing. While Ti- and Ni-based alloys have made rapid progress in AM, the development of AM with Al-alloys has been slower, despite their wide industrial adoption for their low density and high strength-to-weight ratio. The review focuses on microstructural characteristics, their influence on mechanical properties, and recent research on overcoming challenges associated with high-strength wrought Al-alloys in AM. The paper highlights the promising advancements in understanding microstructure and defect formation, along with potential microstructural modification methodologies, while acknowledging the remaining chal-

lenges in this field. Therefore, with the aim of obtaining high mechanical properties, wear resistance and low-cost Al-Fe-Si and Al-Fe-Cr alloys, this study presents a comparative investigation of the tribological behaviour and microstructural characteristics of two different alloys, namely 77.3 % Al-1.8 % Fe-16.7 % Si and 54.1 % Al-12.8 % Fe-27.8 % Cr.

EXPERIMENTAL TECHNIQUES

Sample preparation

The Al-Fe-Cr and Al-Fe-Si alloys of samples were meticulously prepared by controlling the alloy composition. Stir casting techniques were used to fabricate the desired alloy, followed by heat treatment to achieve the desired microstructure and mechanical properties. The experimental data obtained from different tests as shown in Fig. 1 were subjected to rigorous statistical analysis. This comprehensive analysis allowed for comparisons between samples (Al-Fe-Si) and (Al-Fe-Cr) alloys in different concentrations and testing conditions, enabling the identification of significant trends and correlations.

Figure 1. (a) Turing machine section to prepare specimen; (b) microbalance 120 gr. d = 0.1 mg capacity; (c) surface roughness tester; (d) micro test machine; (e) grinder polisher; (f) wavelength dispersive XRF spectrometer; (g) scanning electron microscope (SEM); (h) optical micrograph.

DATA ANALYSIS

Microstructural analysis

Comprehensive microstructural analysis is conducted using advanced techniques such as optical micrograph, scanning electron microscopy (SEM) and wavelength dispersive (XRF) spectrometer. This analysis provided valuable insights into the crystallography and microstructural features of the alloy, offering an understanding of their influence on tribological behaviour.

The optical micrographs of the 77.3 % Al-1.8 % Fe-16.7 % Si alloy as shown in Fig. 2 reveal important details

about its internal microstructure and the presence of various phases, such as aluminium, iron, and silicon phases. The optical micrographs show the arrangement and size of grains in the alloy. The grains appear to have a well-defined and uniform distribution, suggesting a relatively homogenous microstructure. The presence of distinct grain boundaries indicates the formation of individual grains during the alloy's solidification process.

The microstructure for the 90 % Al-5 % Fe-5 % Cr alloy provides valuable information for comparison with the 77.3 % Al-1.8 % Fe-16.7 % Si alloy. Figure 3 reveals the arrangement and size of grains in the 90 % Al-5 % Fe-5 %

Cr alloy. The grains appear to have a defined and uniform distribution, indicating a reasonably homogeneous microstructure. The presence of distinct grain boundaries indicates the formation of individual grains during the alloy's solidification process. The presence of various phases, such as aluminium, iron, and chromium phases, contributes to the alloy's overall properties and behaviour.
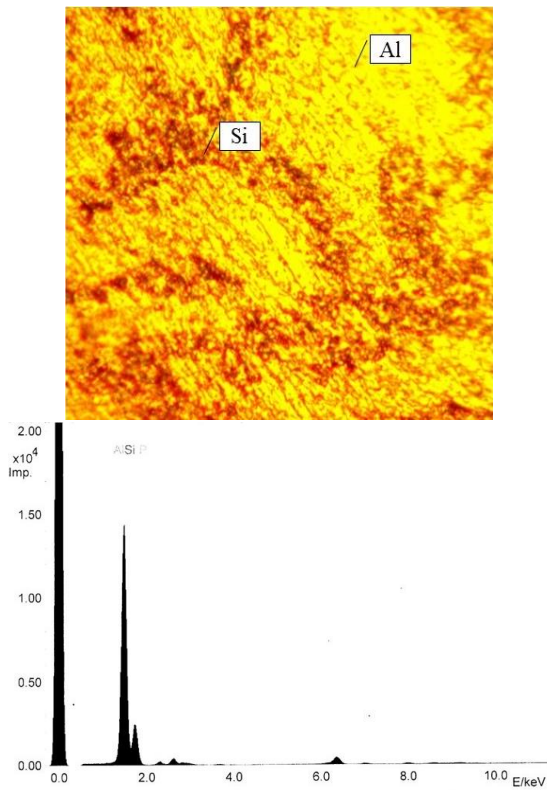
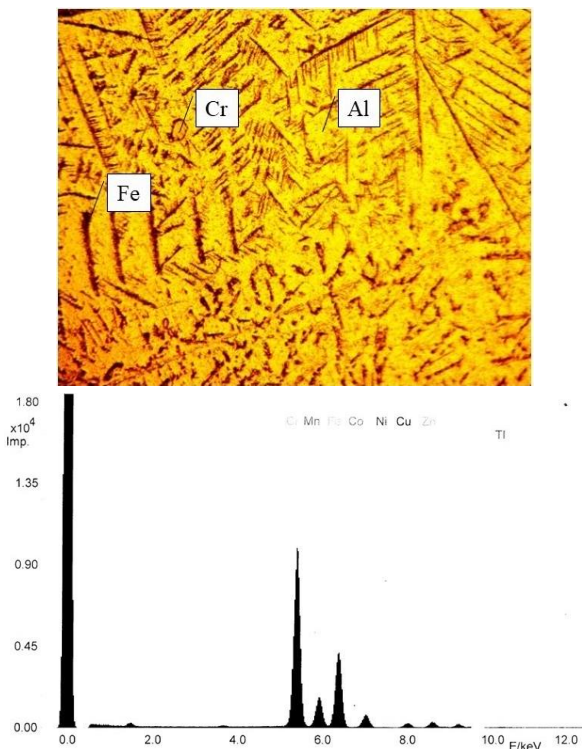Figure 2. Optical micrograph of Al-Fe-Si alloy microstructure.

Figure 3. Optical micrograph of Al-Fe-Cr alloy microstructure.

Hardness testing

To assess the material's resistance to deformation, hardness measurements are carried out using Vickers or Rockwell hardness tests. These measurements provided crucial information related to the alloy's wear resistance. Figure 4 reveals that the Al-Fe-Si alloy exhibits higher Vickers hardness values compared to Al-Fe-Cr alloy, with a difference of approximately 10 degrees between the two specimens.
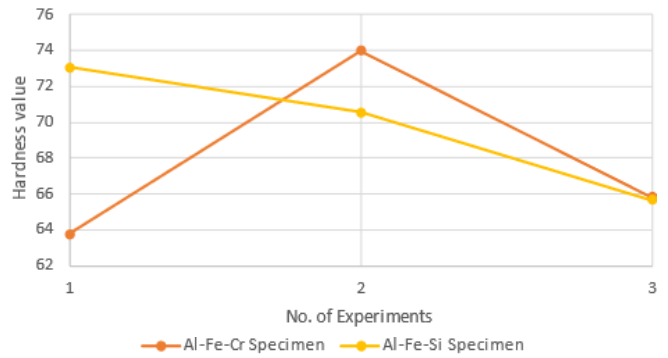
Figure 4. Vicker hardness for Al-Fe-Si and Al-Fe-Cr alloy specimens.

The standard deviation formula can be used to appraise the uniformity or dispersion of Vickers hardness values from a set of height or depth measurements. Here's how you can calculate using the standard deviation formula:

$$\sigma = \sqrt{\frac{\sum[x - \bar{x}]^2}{n}} \ , \qquad (1)$$

where: σ indicates standard deviation; $\sum[x - \bar{x}]^2$ represents the sum of differences between each value in the dataset and mean of all values within that dataset; n is the number of values in the dataset. Table 1 illustrates the standard deviation for each alloy specimen.

Table 1. Standard deviation of specimens.

Specimens	σ
Al-Fe-Cr	4.4099
Al-Fe-Si	3.0735

Tribometer testing

Tribometer testing is performed under controlled conditions to study friction and wear behaviour. Different tribometer setups, such as pin-on-disk, are utilised, varying the loads, sliding speeds, and lubrication conditions. The results demonstrate that the Al-Fe-Si alloy exhibits lower weight loss for all three test loads (3 N, 5 N, and 10 N), whereas the Al-Fe-Cr alloy experiences higher weight loss under the same testing conditions, as shown in Figs. 5 and 6.
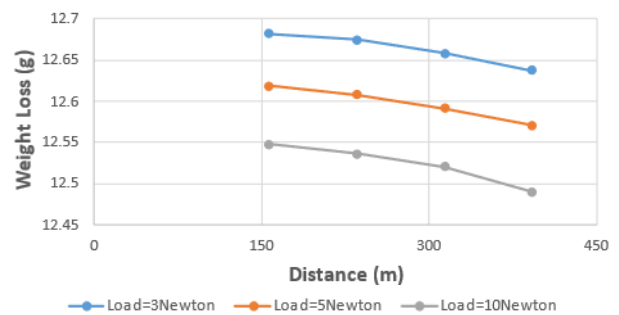
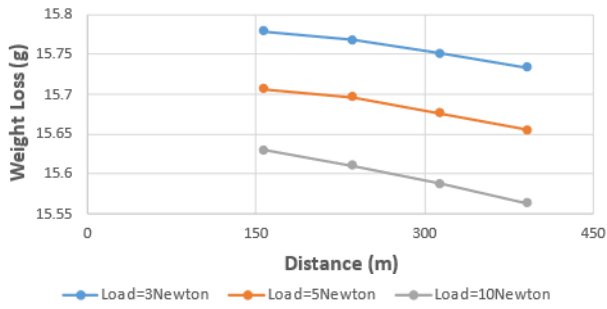Figure 5. Circular wear test for Al-Fe-Si alloy specimen.

Figure 6. Circular wear test for Al-Fe-Cr alloy specimen.

Surface roughness test

In addition to the base alloys testing, researchers explored surface engineering techniques. Surface roughness tests were performed on Al-Fe-Cr and Al-Fe-Si alloys, and the results indicate that the Al-Fe-Si alloy has higher surface roughness values, while the Al-Fe-Cr alloy exhibits lower and more stable roughness levels as shown in Table 2.

Table 2. Surface roughness (R_a) for two alloys specimen.

No. of experiment	Al-Fe-Cr specimen R_a (mm)	Al-Fe-Si specimen R_a (mm)
1	0.108	0.876
2	0.147	0.202
3	0.102	0.237

Scanning electron microscopy (SEM)

The SEM images provided valuable information about the microstructure of the alloy, showing the arrangement and size of grains. The presence of different phases and grain boundaries can influence the alloy's mechanical properties, such as hardness and strength.

The SEM images in Fig. 7 reveal distinct wear patterns on the alloy's surface. These wear features include abrasion marks, grooves, and micro-fractures, indicating the effects of frictional forces during tribological tests. The wear resistance of the alloy appeared to be promising, as it showed limited wear damage and maintained its integrity under the specific test conditions. Also, the analysis allowed for the detection and characterisation of small cracks that had formed on the surface of the alloy. These cracks might have resulted from cyclic loading or localised stress concentration during tribological tests. The presence of such microcracks did not seem to compromise the overall structural integrity of the alloy.
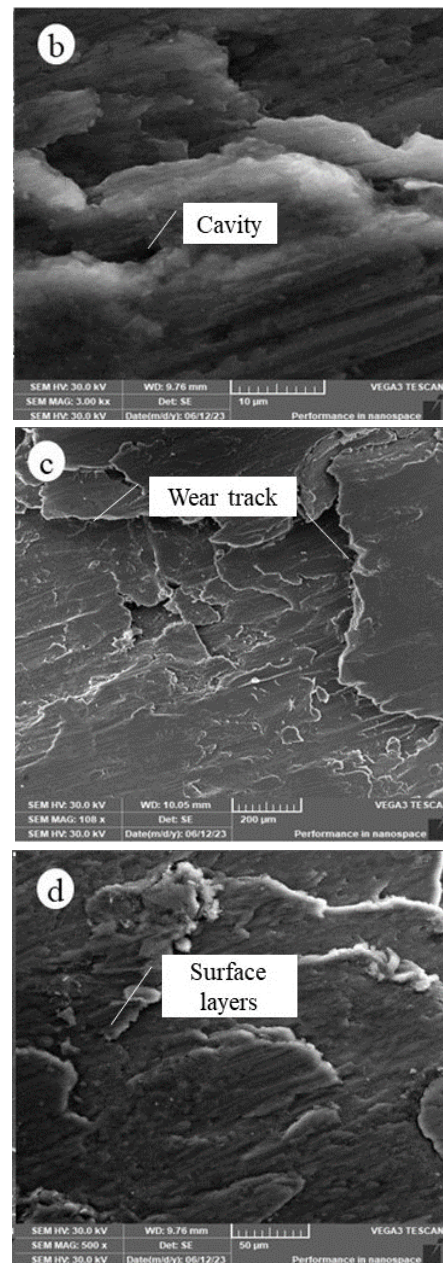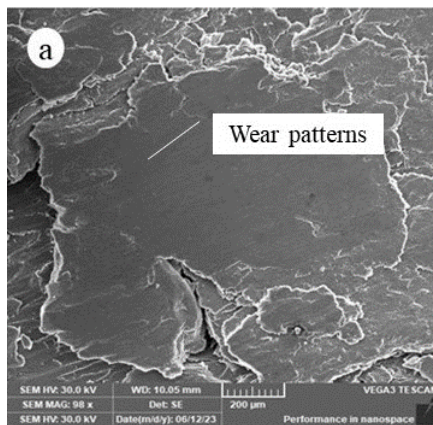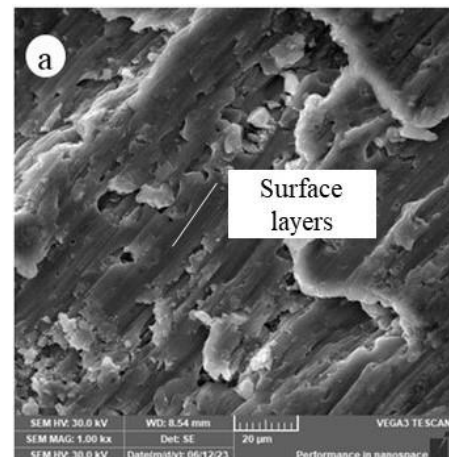

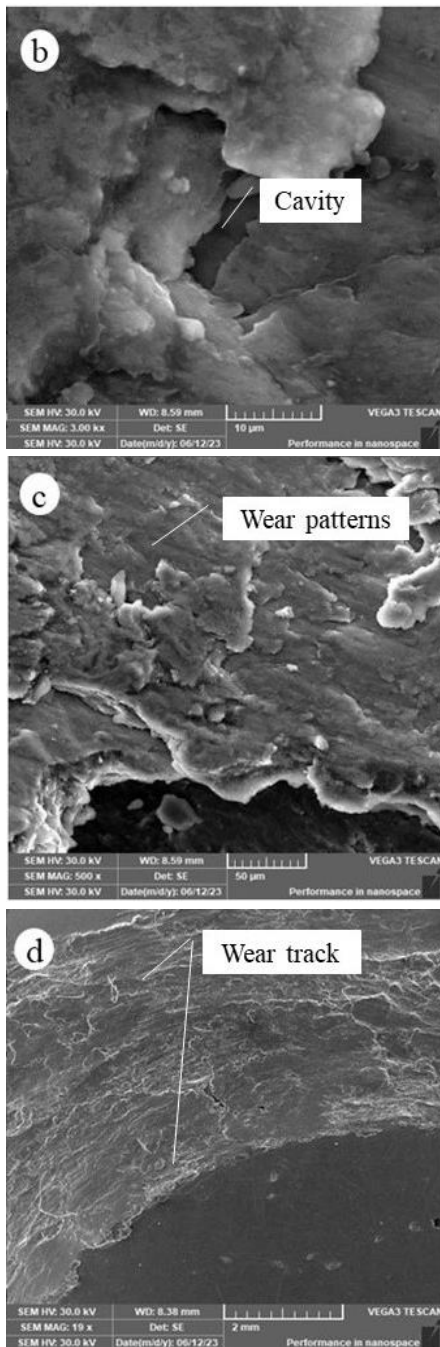Figure 7. SEM micrographs of Al-Fe-Si alloy specimen.

Figure 8. SEM micrographs of Al-Fe-Cr alloy specimen.

The SEM images also show the presence of minor cavity zones or voids on the alloy's surface as in Fig. 8. These cavities may have resulted from material deformation or the presence of impurities. However, they did not appear to have a significant impact on the alloy's mechanical properties, indicating its reasonable ductility and ability to withstand deformation.

CONCLUSIONS

The experimental analysis conducted on two different alloys, 77.3 % Al-1.8 % Fe-16.7 % Si and 90 % Al-5 % Fe-5 % Cr, reveals significant differences in their tribological properties. Investigation involved SEM and optical microscopy of the microstructure to identify wear, crack, and cavity

zones. The Vickers hardness test indicates that the 77.3 % Al-1.8 % Fe-16.7 % Si alloy exhibits higher values, while the 54.1 % Al-12.8 % Fe-27.8 % Cr alloy shows lower hardness, approximately 10 degrees lower.

Furthermore, in the circular wear tests conducted with different loads (3, 5, and 10 N, the 77.3 % Al-1.8 % Fe-16.7 % Si alloy demonstrates less weight loss compared to the 90 % Al-5 % Fe-5 % Cr alloy. This suggests that the former alloy has superior wear resistance under varying loads. Additionally, the roughness test results also favoured the 77.3 % Al-1.8 % Fe-16.7 % Si alloy, showing higher values compared to the 54.1 % Al-12.7 % Fe-27.8 % Cr alloy, which exhibited lower and stable roughness.

Overall, the experimental findings indicate that the 77.3 % Al-1.8 % Fe-16.7 % Si alloy outperforms the 54.1 % Al-12.8 % Fe-27.8 % Cr alloy in terms of hardness, wear resistance, and roughness. These results highlight the potential superiority of the first alloy, suggesting its suitability for applications requiring enhanced tribological properties. However, further investigations and tests may be required to gain a more comprehensive understanding of the alloys' behaviour under various conditions and loads, paving the way for potential engineering applications and industrial usage. The experiment could be extended to include surface modification techniques, such as coatings or treatments, to enhance the alloys' wear resistance and reduce weight loss during wear tests. This would open up possibilities for tailoring the alloys for specific applications.

REFERENCES

1. Aranda, V.A., Figueroa, I.A., González, G., et al. (2021), *Study of the microstructure and mechanical properties of Al-Si-Fe with additions of chromium by suction casting*, J Alloys Comp. 853: 157155. doi: 10.1016/j.jallcom.2020.157155

2. Azadi, M., Azadi, M. (2022), *Data analysis for investigating the tribological behaviors of aluminum-silicon alloys*, Data Brief, 42: 108260. doi: 10.1016/j.dib.2022.108260

3. Farsi, C., Amroune, S., Moussaoui, M., et al. (2019), *High-gradient magnetic separation method for weakly magnetic particles: An industrial application*, Metallofiz. Noveishie Tekhnol. 41(8): 1103-1119. doi: 10.15407/mfint.41.08.1103

4. Al-Abboodi, H., Fan, H., Al-Bahrani, M., et al. (2024), *Mechanical characteristics of nano-crystalline material in metallic glass formers*, Facta Univ.-Ser. Mech. Eng. 22(2): 315-328. doi: 10.22190/FUME230128016A

5. Aldeen, A.W., Mahdi, D.Y., Zhongwei, C., et al. (2024), *Effect of isothermal and isochronal aging on the microstructure and precipitate evolution in beta-quenched N36 zirconium alloy*, Facta Univ.-Ser. Mech. Eng. (online first). doi: 10.22190/FUME230405019A

6. Kang, N., Zhang, Y., El Mansori, M., & Lin, X. (2023), *Laser powder bed fusion of a novel high-strength quasicrystalline Al-Fe-Cr reinforced Al matrix composite*, Adv. Powder Mater. 2(2): 100108. doi: 10.1016/j.apmate.2022.100108

7. Zhang, Y., Kang, N., EL. Mansori, M., et al. (2023), *Friction and dry sliding wear of Al-Fe-Cr quasicrystals with multi-reinforcements by laser powder bed fusion*, Wear, 522: 204682. doi: 10.1016/j.wear.2023.204682

8. Blakey-Milner, B., Gradl, P., Snedden, G., et al. (2021), *Metal additive manufacturing in aerospace: A review*, Mater. Des. 209: 110008. doi: 10.1016/j.matdes.2021.110008

9. Leyson, G.P.M., Hector Jr., L.G., Curtin, W.A. (2012), *Solute strengthening from first principles and application to aluminum*

alloys, Acta Mater. 60(9): 3873-3884. doi: 10.1016/j.actamat.2012.03.037

10. Xi, L.X., Zhang, H., Wang, P., et al. (2018), *Comparative investigation of microstructure, mechanical properties and strengthening mechanisms of Al-12Si/TiB$_2$ fabricated by selective laser melting and hot pressing*, Ceram. Int. 44(15): 17635-17642. doi: 10.1016/j.ceramint.2018.06.225

11. Kang, N., El Mansori, M., Lin, X., et al. (2018), *In-situ synthesis of aluminum/nano-quasicrystalline Al-Fe-Cr composite by using selective laser melting*, Composites Part B: Eng. 155: 382-390. doi: 10.1016/j.compositesb.2018.08.108

12. Wang, X., Guan, R.G., Wang, Y., et al. (2019), *Mechanistic understanding on the evolution of nanosized Al$_3$Fe phase in Al-Fe alloy during heat treatment and its effect on mechanical properties*, Mater. Sci. Eng. A, 751: 23-34. doi: 10.1016/j.msea.2019.02.066

13. Khadem, M., Penkov, O.V., Yang, H.-K., Kim, D.-E. (2017), *Tribology of multilayer coatings for wear reduction: A review*, Friction, 5(3): 248-262. doi: 10.1007/s40544-017-0181-7

14. Aversa, A., Marchese, G., Saboori, A., et al. (2019), *New aluminum alloys specifically designed for laser powder bed fusion: A review*, Materials, 12(7): 1007. doi: 10.3390/ma12071007

15. Kotadia, H.R., Gibbons, G., Das, A., Howes, P.D. (2021), *A review of laser powder bed fusion additive manufacturing of aluminium alloys: Microstructure and properties*, Add. Manuf. 46: 102155. doi: 10.1016/j.addma.2021.102155